Calcium Transfer to Oxide Inclusions in Al-Killed Steel Without Calcium Treatment

DEEPOO KUMAR and PETRUS CHRISTIAAN PISTORIUS

Alumina inclusions generated from aluminum deoxidation may undergo several transformations depending on steelmaking conditions. Under reducing conditions, in contact with MgO-saturated slag, alumina inclusions are known to transform to spinel. However, there are uncertainties related to CaO pick-up by alumina-based inclusions. This work aims to provide some clarification of CaO pick-up by alumina inclusions through a series of experiments. First, the role of silicon in calcium transfer from slag was examined by conducting two similar experiments: one without any silicon addition and a second with 1 wt pct electronic grade silicon addition. Second, the role of crucibles was tested by conducting experiments in ZrO_2 and CaO-3 pct ZrO_2 crucibles. It was found that the addition of silicon significantly enhances the rate of CaO pick-up when there was no silica in the slag at the start of reaction. The effect of the crucible on CaO pick-up was found to be weaker than that of the 1 wt pct silicon addition.

https://doi.org/10.1007/s11663-020-02004-6

I. INTRODUCTION

In aluminum-killed steel covered with MgO-saturated slag (as is common in secondary metallurgy), alumina inclusions pick up magnesium, with simultaneous reduction of Al_2O_3 from the inclusions. These reactions transform the inclusions from alumina to spinel (solid solution based on $MgO.Al_2O_3$) and eventually to MgO.[1] The source of magnesium is reduction of MgO from the slag. It was shown that the rate of magnesium pick-up by the inclusions (and by the steel) can be modeled by assuming control by mass transfer in the steel to the steel–slag interface, with local equilibrium at that interface.[2,3] In principle, calcium pick-up can occur in the same way, since ladle slags are commonly at or near saturation with calcium oxide: aluminum can reduce some calcium oxide from the slag, dissolving calcium in the steel to react with inclusions. However, under carefully controlled laboratory conditions, the rate of transfer of calcium is much lower than that of magnesium.[2] Recent work indicated that this difference in rate is the result of the difference in the oxygen affinity of calcium and magnesium (CaO is much more stable than MgO) and weak interaction between dissolved calcium and dissolved oxygen in the steel (much weaker than previous solution models indicated).[4] Weak interaction between calcium and oxygen contributes to low concentrations of dissolved calcium.

However, another possible contributor to slow calcium pick-up under laboratory conditions is reaction with the crucible. If a magnesium oxide crucible is used, some dissolved aluminum is consumed by pick-up of Mg from the crucible, in parallel with slag reduction; reduction of MgO would compete with CaO reduction (by consuming dissolved aluminum), limiting Ca pick-up by the steel and inclusions. Kinetic considerations indicate that this effect would be weak: the rates of Mg and Ca pick-up (by steel and inclusions) are limited by mass transfer of dissolved Mg and Ca (at typical concentrations of a few parts per million or less) and not by mass transfer of Al (typical concentration hundreds of parts per million). However, to test for possible unanticipated effects, in this work several different crucibles were tested experimentally: MgO, ZrO_2, and CaO-3 pct ZrO_2.

Industrial observations indicate that silicon-rich steels pick up calcium more readily during ladle treatment, than steels with low silicon concentrations.[5] This might be caused by calcium contained in ferrosilicon (that is commonly added to steel to increase the silicon concentration of the steel). However, to test for possible additional effects of Si in solution in steel, in this work steel–slag experiments were conducted with zero and 1 pct Si in the liquid steel.

DEEPOO KUMAR and PETRUS CHRISTIAAN PISTORIUS are with the Center for Iron and Steelmaking Research, Department of Materials Science and Engineering, Carnegie Mellon University, 5000 Forbes Avenue, Pittsburgh, PA 15213 Contact e-mail: pistorius@cmu.edu
Manuscript submitted 24 August 2020; accepted 09 October 2020.
Article published online November 2, 2020.

II. EXPERIMENTAL

Experiments were conducted in a laboratory induction furnace, as described elsewhere.[6,7] Changes in inclusions were tracked by taking liquid steel samples (as described previously[6,7]). Samples were mounted in resin, ground, and polished to a 1-μm finish (using diamond suspension). Automated inclusion analysis was performed with an FEI/ASPEX Explorer scanning electron microscope (SEM) at 10 kV, analyzing an area of approximately 10 mm^2 on each sample. Other instrument settings were as described elsewhere[8] yielding a spatial resolution of approximately 0.3 μm.

Two experiments were conducted using MgO crucibles, testing the effect of Si alloying. Each used 600 g of low-sulfur (8 ppm) electrolytic iron and 160-170 g slag (composition in Table I) melted in an MgO crucible with the composition and size used in previous work[6] (internal diameter approximately 50 mm), in an argon atmosphere. The slag composition was chosen to be doubly saturated with the lime (CaO-based) and periclase (MgO-based) solid solutions, based on FactSage equilibrium calculations (FactSage 7.3, FToxid database). The electrolytic iron was mixed with the premelted $CaO-Al_2O_3$-MgO slag and heated to the test temperature of 1600 °C. Aluminum (0.3 wt pct of the iron mass) was added to the molten mixture approximately 15 minutes after it reached the test temperature. Aluminum was added in the form of shot wrapped in iron foil, and attached to the end of an alumina rod for immersion into the steel. The aluminum deoxidation step was defined as $t = 0$ minutes for the experiments. Based on previous experiments, addition of 0.3 pct Al would have resulted in approximately 0.26 pct dissolved Al. In one experiment, 1 pct silicon was added as electronics grade Si at $t = 5$ minutes. The addition and sampling details for the two experiments are given by Tables II and III. Samples were taken by aspirating steel into a fused-quartz tube (4 mm ID), using a pipette pump. The "SF" sample was taken from the solidified steel "puck" that remained in the crucible after the experiment.

Steel–slag reactions without any intentional MgO addition were conducted using ZrO_2 crucibles of 39 mm inner diameter. Solid electrolytic iron (7 ppm S; 100 g) was melted and deoxidized by adding 0.15 pct Al; 30 g of slag (see chemistry in Table IV; near CaO saturation) was added at $t = 6$ minutes, see Table V. ZrO_2 (2 pct of slag mass) was added in the slag to limit corrosion of the crucible.

Two experiments were conducted using Al-killed steel in a 40-mm inner diameter CaO-3 pct ZrO_2 crucible (supplied by Zhengzhou Mission Ceramic Products Co, Ltd, Zhengzhou, China). One experiment was conducted using 250 g of electrolytic iron (containing 40 ppm of sulfur and approximately 360 ppm of oxygen) with 50 g of $CaO-Al_2O_3$ slag near CaO saturation

Table I. Composition of Slag 1, Used to Test the Effect of Silicon on Calcium Transfer (Mass Percentages)

Pct CaO	Pct Al_2O_3	Pct MgO	Pct SiO_2
51	42	7	0

Table II. Addition and Sampling Schedule for Si-Free Al-Killed Steel Reacted with Slag in an MgO Crucible (Steel Mass = 600 g, Slag Mass = 170 g)

Time (min)	0	1	16	31	70
Event / sample number	0.3Pct Al added	S1	S2	S3	SF

Table III. Addition and Sampling Schedule for Reaction of Al-Killed Steel Containing 1 Pct Si with Slag in an MgO Crucible (Steel Mass = 600 g, Slag Mass = 160 g)

Time (min)	0	5	7	20	35	50	65	75
Event/Sample Number	0.3 pct Al added	1 pct Si added	S1	S2	S3	S4	S5	SF

Table IV. Compositions of MgO-Free Slag Used to Study Steel–Slag Reaction in ZrO_2 and CaO-3 pct ZrO_2 Crucibles

Crucible	Pct CaO	Pct Al_2O_3	Pct ZrO_2
ZrO_2	56	42	2
CaO-3 pct ZrO_2	57	43	0

Table V. Addition and Sampling Details for Reaction of Al-Killed Steel with MgO-Free Slag in a ZrO_2 Crucible

Time (min)	0	6	24	52	68	92
Event/Sample	0.15 pct Al added	30 g slag added	S1	S2	S3	SF

Table VI. Addition and Sampling Detail for Al-Killed Steel Containing Approximately 40 ppm S, Contained in a CaO-3 Pct ZrO_2 Crucible and Reacted with CaO-Al_2O_3 Slag

Time (min)	0	6	13	19	24	34	43	54
Event/Sample	0.16 pct Al added	50 g slag added	S3	S4	S5	S6	S7	S8

Table VII. Addition and Sampling Detail for Al-Killed Steel Containing Approximately 8 ppm S, Contained in a CaO-3 Pct ZrO_2 Crucible

Time (min)	0	4	15	30	45
Event/Sample	0.15 pct Al added	S2	S3	S4	S5

(Table VI) (addition and sampling details in Table VI). The other experiment used 200 g of low-sulfur electrolytic iron (8 ppm S) with no slag addition (addition and sampling details in Table VII).

III. RESULTS AND DISCUSSION

A. *Effect of Silicon Addition on Calcium Transfer*

The inclusions in Al-killed steel that did not contain Si followed the familiar transformation from alumina to spinel, and finally to MgO,[9,10] with very little calcium transfer (Figure 1). Transformation was rapid, due to the relatively high Al concentration (0.3 pct) and the presence of slag at the steel–crucible interface (Figure 2); the slag avoided the formation of a spinel layer which would have slowed down magnesium pick-up from the crucible.[9]

The observed increase of alumina in inclusions from S2 (t = 16 minutes) to S3 (31 minutes) apparently reflects minor reoxidation of the melt that generated fresh Al-Mg-O inclusions and a small increase in the area fraction of inclusions. Most inclusions in the final sample (70 minutes) were MgO with limited calcium. Figure 3 shows such a calcium-containing inclusion: the inclusion was mainly MgO with small amount of calcium sulfide.

In contrast, the steel that contained 1 pct Si did show significant calcium pick-up (Figure 4). The inclusions in the first sample were spinel and spinel-MgO combinations, with a minor concentration of CaO in a few. From the second sample, the inclusions contained more calcium, with a few falling in the calcium corner of the ternary diagram (representing CaS) (see Figure 4(b)). The third sample indicated continued pick up of calcium and a lower magnesium concentration in inclusions, indicating that calcium from steel–slag reaction may have reduced MgO at the steel–inclusion interface as proposed by Yang *et al.*[11] The inclusions in this sample were mixtures of liquid or partially liquid CaO-Al_2O_3-MgO inclusions and MgO-rich MgO-Al_2O_3 inclusions. Similar inclusions were found in the samples taken later (S4 and S5, Figures 4(d) and (e)). Examples of inclusion micrographs (taken with a higher-resolution field-emission gun SEM) are shown in Figure 5. The inclusions in the final sample (Figure 4(f)) were notably different: mainly MgO-rich inclusions, with some CaO-Al_2O_3-MgO inclusions and occasional MgO-CaS inclusions. The large change from the preceding sample likely resulted from changes during solidification: the last sample was taken from the steel puck that solidified in the crucible, with a much longer solidification time than the 4-mm-diameter samples taken during the experiment; continued supply of magnesium from the crucible and slag, and sulfur removal to the slag, may also have contributed to continued inclusion evolution.

These results do indicate that silicon can promote calcium pick-up by inclusions, perhaps because silicon is a strong deoxidizer if the slag does not contain SiO_2 (as was the case at the start of the experiments). Current results are similar to those showed by Mu *et al.*[10] for modification of alumina/spinel inclusions by calcium transfer from CaO and MgO-saturated slag reacting with steel containing 2 wt pct Al. It should be noted that

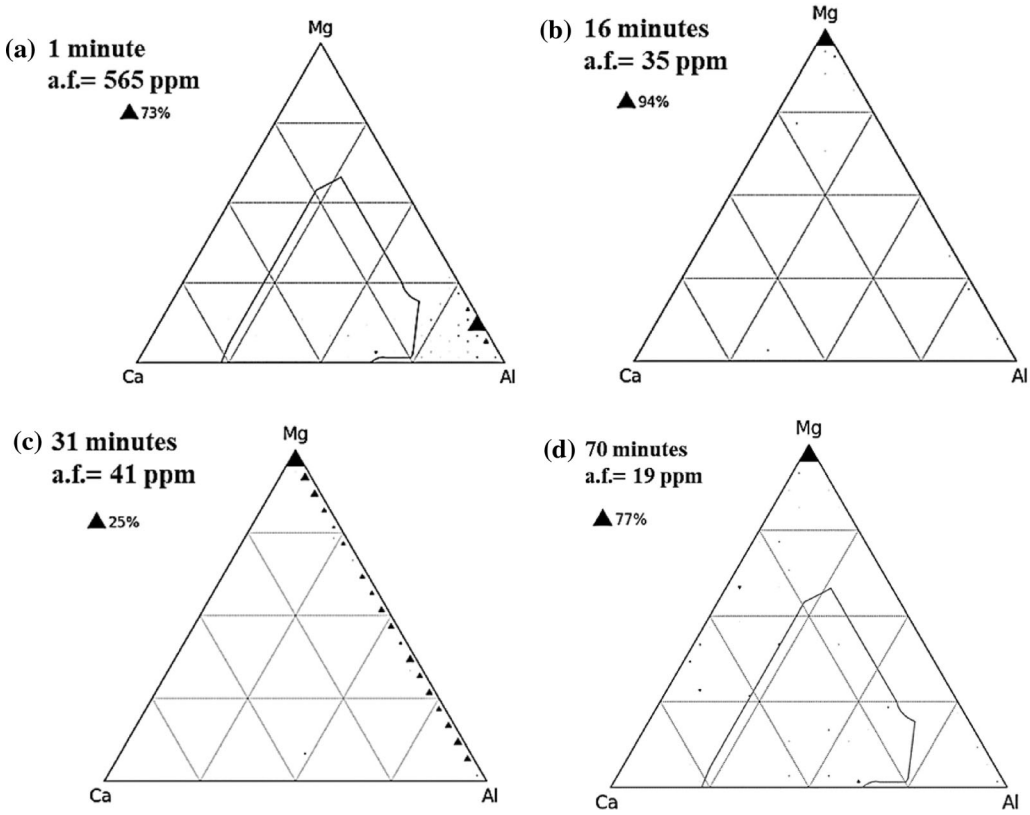

Fig. 1—Inclusion composition in steel samples taken at (*a*) 1 min, (*b*) 16 min, (*c*) 30 min, and (*d*) 70 min after Al addition, for reaction of Si-free Al-killed steel with $CaO\text{-}Al_2O_3\text{-}MgO$ slag. (The lines in (*a*) and (*d*) indicate the boundary of inclusions that would be 50 pct liquid at 1550 °C; ''a.f.'' is the area fraction of inclusions.).

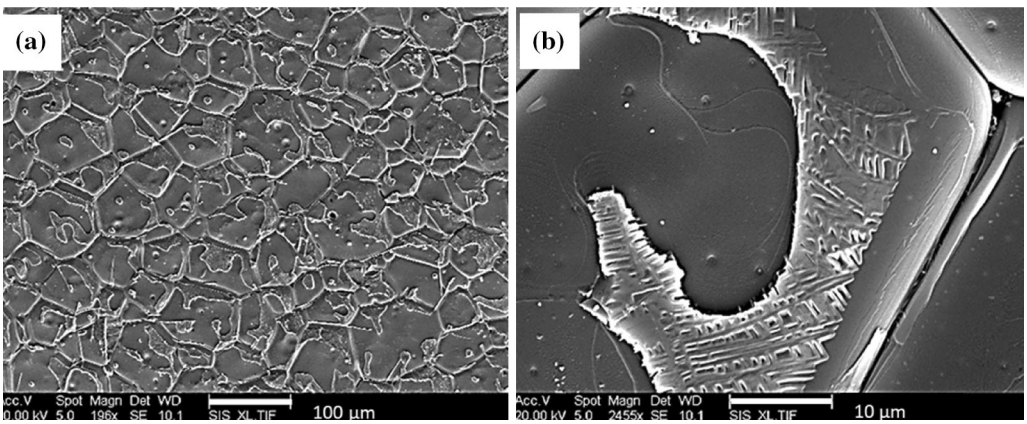

Fig. 2—MgO crucible inner wall coated with slag after reaction of Si-free steel with $CaO\text{-}Al_2O_3\text{-}MgO$ slag. Secondary electron micrographs, shown at (*a*) lower and (*b*) higher magnifications.

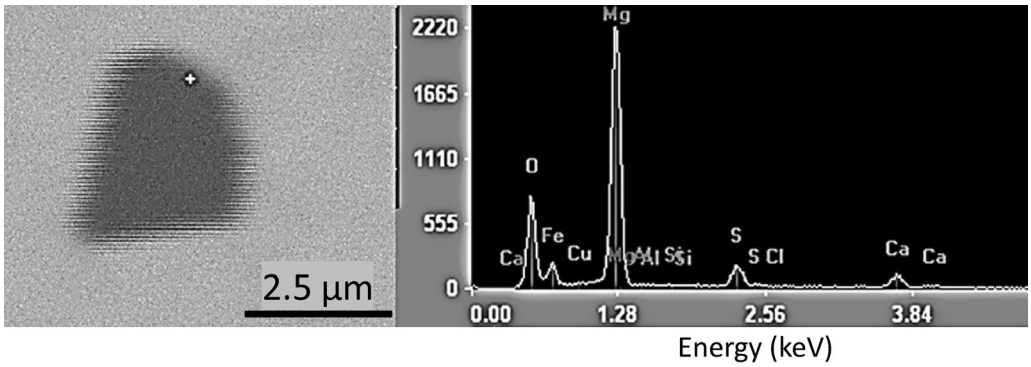

Fig. 3—MgO-CaS inclusion in final steel sample ("SF") after 75 min of reaction of Si-free 0.3 pct Al steel with CaO-Al_2O_3-MgO slag. Backscattered electron micrograph with EDX spectrum measured at the point indicated with a cross.

much lower calcium transfer to inclusions was observed for experiments conducted with lower Al additions (0.1, 0.5, and 1 wt pct) in that study.

To evaluate the reduction effect of added silicon, the equilibrium steel compositions were calculated for the two cases (0.3 pct Al added, to iron with zero or 1 pct Si), after reaction with slag as listed in Table I, using the steel and slag masses as stated in Tables II and III. FactSage 8.0 was used[12] (FToxid slag and solid-oxide models, and FSstel liquid steel model, with the Ca*O associate suppressed).[4] In the Si-bearing case, some reduction of Al_2O_3 from the slag was predicted, with the slag containing approximately 1 pct SiO_2 at equilibrium. The corresponding steel compositions are listed in Table VIII, indicating that the more-reducing conditions (resulting from the addition of Si) did give higher equilibrium concentrations of Al, Ca, and Mg in the steel. However, the Ca concentration is predicted to increase by a factor of two only (comparing Si-alloyed steel with Si-free steel), which appears too small to account for the observed much more extensive calcium transfer to inclusions (by a factor of approximately thirty), in the Si-alloyed steel. The average composition of inclusions in the second sample taken at 15-20 minutes, in the two experiments are shown in Table IX showing significantly higher CaO concentration in inclusions due to silicon alloying. Rather, it is possible that the reaction between silicon (in the steel) and alumina (in the slag) may have resulted in slag emulsification. Such emulsification would increase the slag–steel contact area, and could also transfer calcium aluminate droplets as inclusions into the steel. Emulsification at the slag–steel interface during redox reactions has been documented in the past, and recently reviewed and modeled by Spooner *et al.*[13]

B. *Effect of Crucible: ZrO_2 and CaO-ZrO_2*

1. *ZrO_2 crucible*

In the ZrO_2-crucible test, Al-killed steel was in contact with CaO-Al_2O_3 slag (containing no added MgO). The slag was kept MgO-free to avoid the possible competition between Mg and Ca pick-up at the steel–slag interface. Analysis of inclusions in samples S1 (24 minutes after deoxidation) and SF (92 minutes) are shown in Figures 6(a) through (d). For each sample, compositions are plotted on two ternary diagrams: Al-Mg-Ca and Al-Mg-Zr. Two types of inclusions were found in these samples: ZrO_2-rich inclusions (Type 1) and Al_2O_3-rich inclusions (Type 2). Examples of both types are shown in Figure 7 and their main characteristics are summarized in Table X. Note that some MgO pick-up was found; possible sources of magnesium are discussed later.

Automated inclusion analysis was affected by the presence of the ZrO_2-rich phase that appeared bright (because of its high average atomic number, see Figure 7(a)). Typically, during automated analysis possible inclusions are identified by lower backscattered electron yield (appearing darker). It is likely that some (bright) ZrO_2-rich inclusions were missed during automated analysis of these samples.

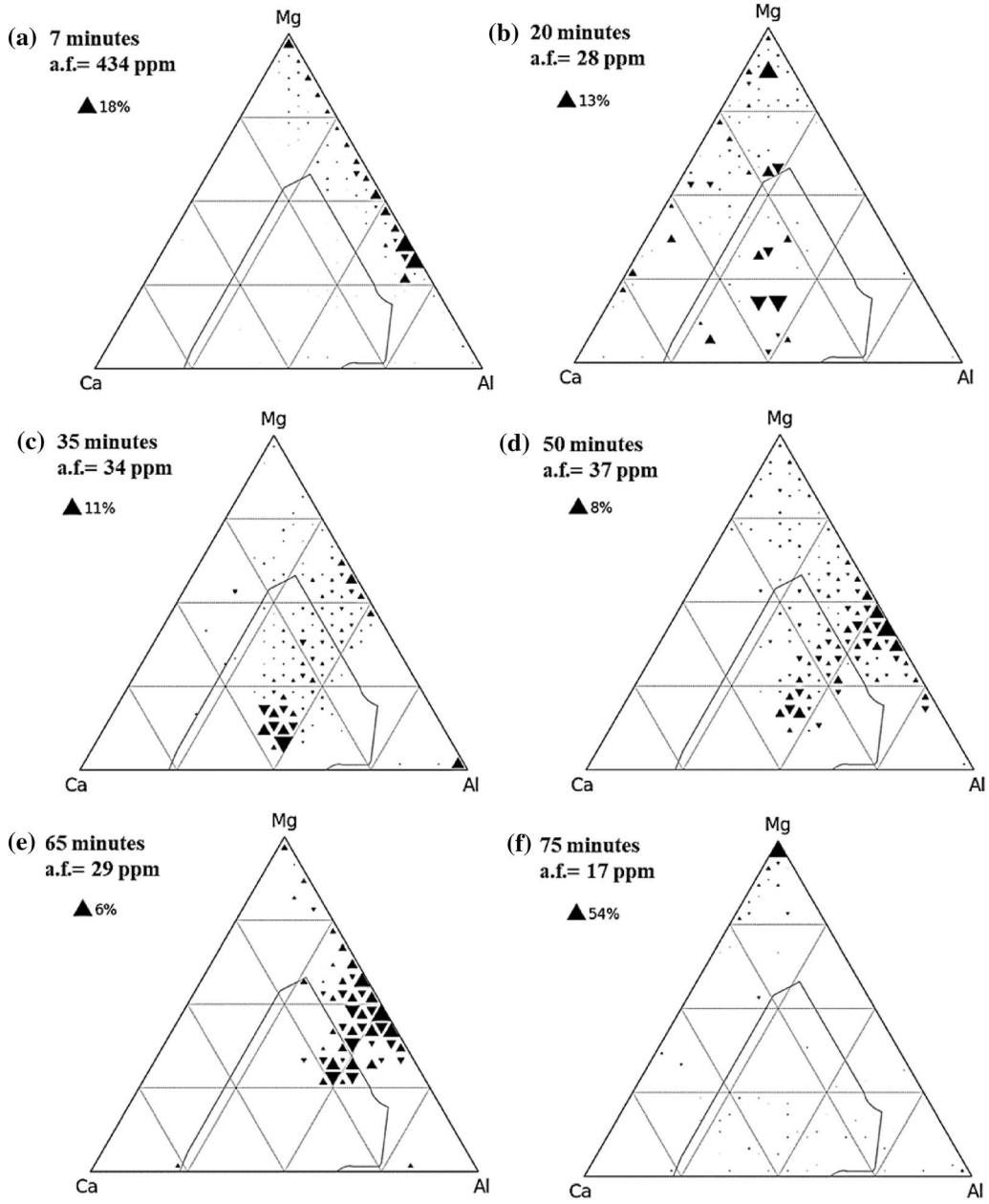

Fig. 4—Inclusion composition for experiment with 0.3 pct Al and 1 pct Si after (*a*) 7 min, (*b*) 20 min, (*c*) 35 min, (*d*) 50 min, (*e*) 65 min, and (*f*) 75 min after Al addition. (The lines indicate the boundary of inclusions that would be 50 pct liquid at 1550 °C.).

The measurable calcium content in the ZrO_2-rich phase of some type 1 inclusions indicates that these may have resulted from slag–crucible reaction, forming calcium zirconate that may have eroded into the steel melt subsequently. As the $CaO-ZrO_2-AlO_{1.5}$ phase diagram in Figure 8 shows, calcium zirconate ($CaZrO_3$) is the expected product if CaO-rich $CaO-Al_2O_3$ slag reacts with ZrO_2. Whether these inclusions formed by transfer of dissolved calcium or of calcium zirconate, in all cases the extent of calcium pick-up by inclusions was very limited (Figure 6). The observed behavior is not much different than that found in similar experiments done earlier using MgO crucibles.[2] In those experiments, alumina inclusions quickly transformed to spinel inclusions picking up Mg from the crucible and the slag. There was no observable calcium pick-up.

Fines from direct erosion of the ZrO_2 crucible also appeared to contribute to the formation of the Type 1 inclusions. The example in Figure 9 indicates that MgO and Al_2O_3 precipitated on ZrO_2. Equilibrium calculations (with FactSage) confirmed that formation of Al_2O_3 by reaction of 0.15 pct Al steel with ZrO_2 is possible.

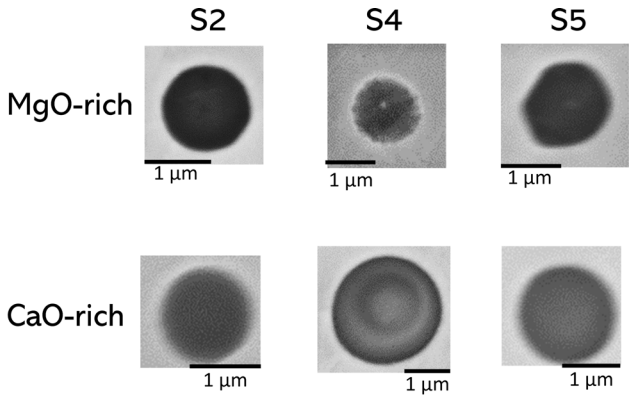

Fig. 5—Examples of MgO-rich and CaO-rich inclusions observed in samples taking at different times during reaction of Si-alloyed Al-killed steel with $CaO-Al_2O_3$-MgO slag.

Examination of the inner wall of the crucible after experiments clearly showed slag attack on the crucible (Figure 10).

Even though the slag and crucible did not contain any MgO, MgO was detected in the inclusions. Analysis of the crucible before and after the experiment found little evidence of MgO except for a Si-Ca-Mg-Al-O fiber on the crucible wall after the experiment (Figure 11). The most likely source of such fibers is paper used in wrapping the crucibles for shipping, or used during experimental setup. Because of the low total inclusion concentration in the steel for these experiments, even a small amount of contamination would have affected the measured inclusion composition: In total, the steel contained only ~0.1 ppm of MgO (in inclusions), equivalent to 10 μg of MgO (Figure 6).

2. *CaO-3 pct ZrO_2 crucible*

After reaction of Al-killed steel with $CaO-Al_2O_3$ slag in a CaO-3 pct ZrO_2 crucible, the inclusions were alumina + spinel with limited calcium and zirconium contents (see Figure 12). Figure 13 shows a calcium-containing inclusion observed in the sample taken at 34 minutes. The extent of magnesium pick-up in these inclusions was less than in the experiments using MgO and ZrO_2 crucibles. The calcium and zirconium content in inclusions increased slightly with time: The average cation mole fraction of calcium (out of the total of Ca, Mg, Al, Si, and Zr) increased from 0.90 to 3.8 pct from the sample taken at 34 minutes to that taken at 54 minutes, while the area fraction of inclusions decreased from 102 to 28 ppm due to inclusion flotation. Zirconium pick-up in these inclusions was apparently by the reduction of zirconia from the crucible by aluminum from steel.

While 50 g of $CaO-Al_2O_3$ slag had been added at $t = 6$ minutes, at the end of the experiment no slag was observed on top of the solidified steel; the slag had penetrated the crucible (Figure 14).

Slag penetration was characterized by polishing a cross-section of the $CaO-ZrO_2$ crucible after the experiment, using acetone for cleaning during polishing to avoid attack of the crucible by water. Figure 15

Table VIII. Calculated Equilibrium Composition for Reaction of Si-Free and Si-Bearing Steel (Initially Containing 0.3 Pct Al and 400 ppm O) with MgO-Saturated Calcium Aluminate Slag, at 1600 °C

Steel	Pct Al	Pct Si	ppm Mg	ppm Ca	ppm O
Si-free	0.26	0	15.0	0.036	4.6
Si-alloyed	0.43	0.86	19.3	0.071	4.3

Table IX. Inclusion Composition in Second Sample of Heats With and Without Silicon Alloying

Exp.	Sampling time	Pct MgO	Pct CaO	Pct Al_2O_3	Area fraction
No silicon	16 min	95	1	4	35 ppm
With 1 pct silicon	20 min	55	31	14	28 ppm

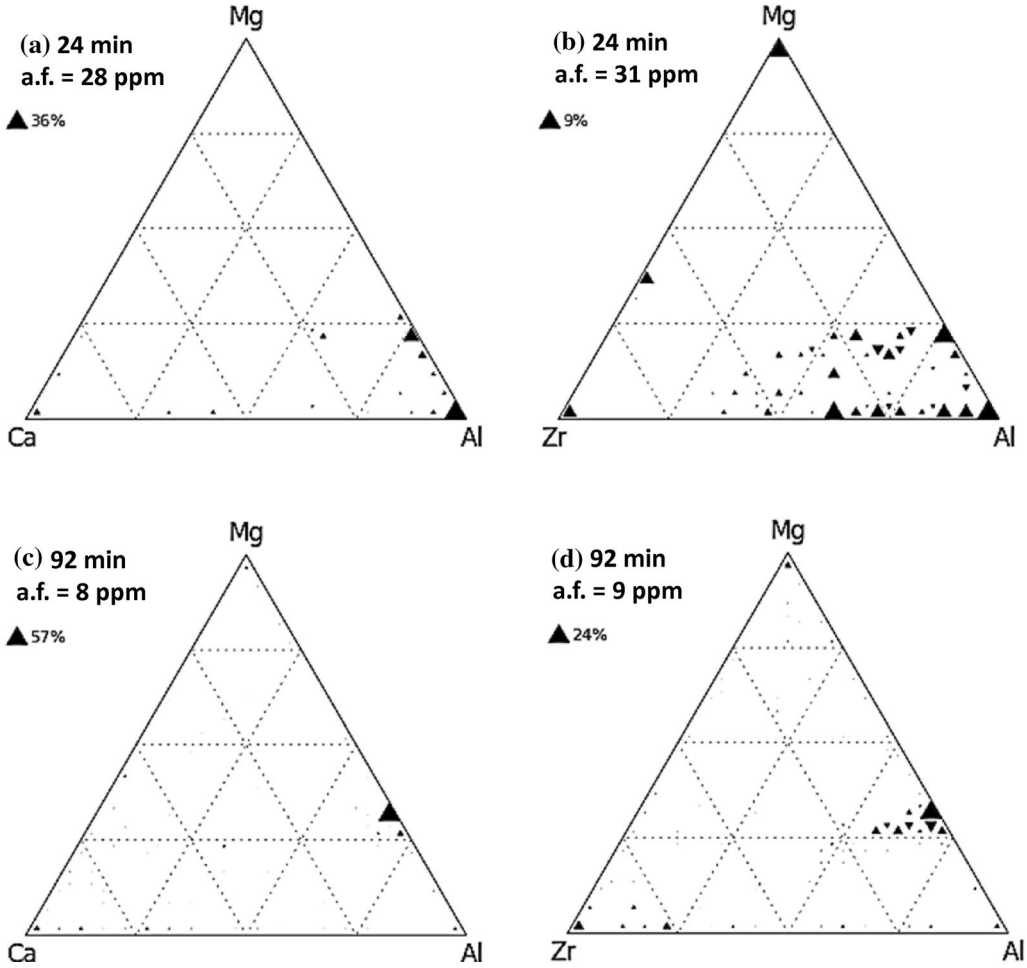

Fig. 6—Inclusion analysis of first (*a* and *b*) and last (*c* and *d*) samples taken during reaction of Al-killed steel with CaO-Al_2O_3 slag in a ZrO_2 crucible. Two ternary diagrams (Ca-Mg-Al and Mg-Zr-Al; plotted as cation mole fractions) are shown for each.

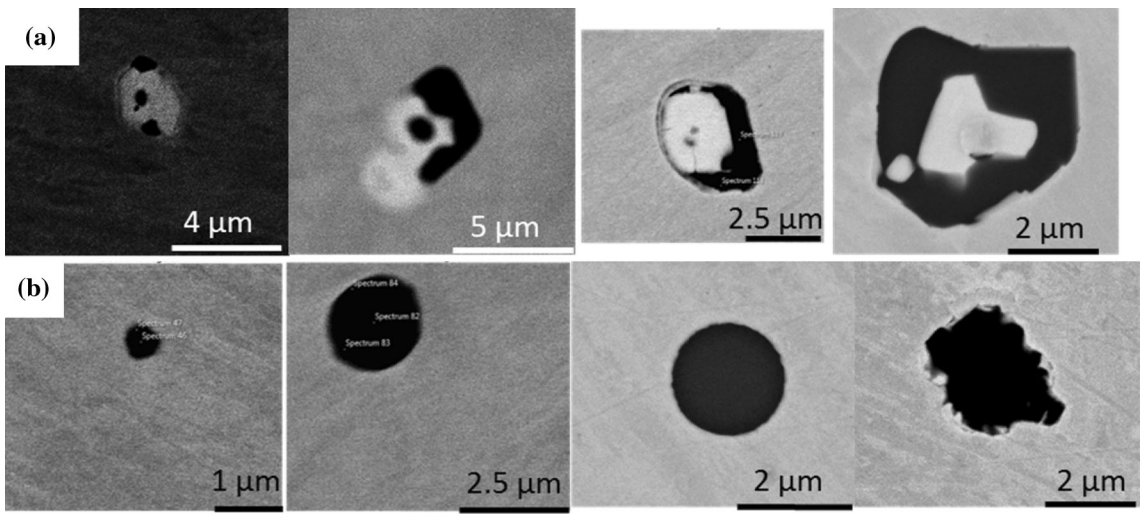

Fig. 7—Examples of inclusions found after reaction of Al-killed steel with CaO-Al_2O_3 slag in a ZrO_2 crucible: (*a*) Type 1 inclusions: combination of a ZrO_2-rich phase (bright) with an Al_2O_3-rich phase; (*b*) Type 2 inclusions: Al_2O_3-rich phase with some MgO, ZrO_2, and CaO. Backscattered electron micrographs.

confirms that slag penetrated along the grain boundaries of the crucible; aluminum is a clear indication of the presence of slag.

Table X. Characteristic of Type 1 and Type 2 Inclusions Found After Reaction of Al-Killed Steel with CaO-Al_2O_3 Slag in a ZrO_2 Crucible

Type 1 (ZrO_2-rich) Inclusions	Type 2 (Al_2O_3-rich) Inclusions
ZrO_2-rich phase: Almost pure ZrO_2, containing less than 2 wt pct each of Al_2O_3 and MgO. CaO content (wt pct) in this phase increased as follows: 0 in S1, <1 in S2, <2 in S3, and <5 in S4.	Most inclusions had a higher ZrO_2 content than the Al_2O_3-rich phase of Type 1 inclusions (>15 wt pct)
Al_2O_3-rich phase: MgO content up to 17 wt pct; ZrO_2 content generally low (<5 wt pct); occasionally higher ZrO_2 content (up to 40 wt pct) was found. For later samples, traces of CaO (<1 wt pct) also found.	MgO content very low compared with the Al_2O_3-rich phase in Type 1 inclusions except for the final sample (S4) where MgO content was around 25 wt pct
	Inclusions in S1 and S2 did not contain any measurable CaO; those in S3 and S4 had a small amount of CaO (<1.5 wt pct)

SEM-EDS analysis of the grain boundary region of the crucible (away from the region with slag penetration) showed the presence of silicon and magnesium as shown in Figure 16. This indicates that the crucible could have been the source of magnesium observed in the inclusions (Figure 12).

More calcium pick-up was observed in the experiment performed without slag (Al-killed steel contained in a CaO-ZrO_2 crucible, Figure 17): After 15 minutes, the inclusions were alumina and spinel with limited calcium and zirconium contents. The calcium and zirconium content in inclusions increased with time; partial calcium modification of spinel inclusions can be observed in the final sample. Figure 18 shows a calcium-containing inclusion observed in the sample taken at the 45th minute. The sample taken after 30 minutes showed an increase in the area fraction of inclusions (from 13 ppm to 95 ppm) and inclusions were alumina rich, indicating reoxidation during sampling; the inclusions in this sample were also higher in silicon. The increase in silicon concentration indicates likely silica contamination by the fused-quartz sampler tube. However, the significant CaO in the inclusions in the subsequent samples indicates continued calcium pick-up by steel–crucible reaction. Calcium pick-up is clearly possible, but to a limited extent; note that the total inclusion concentration (indicated by the area fraction of inclusions) was very low in these experiments.

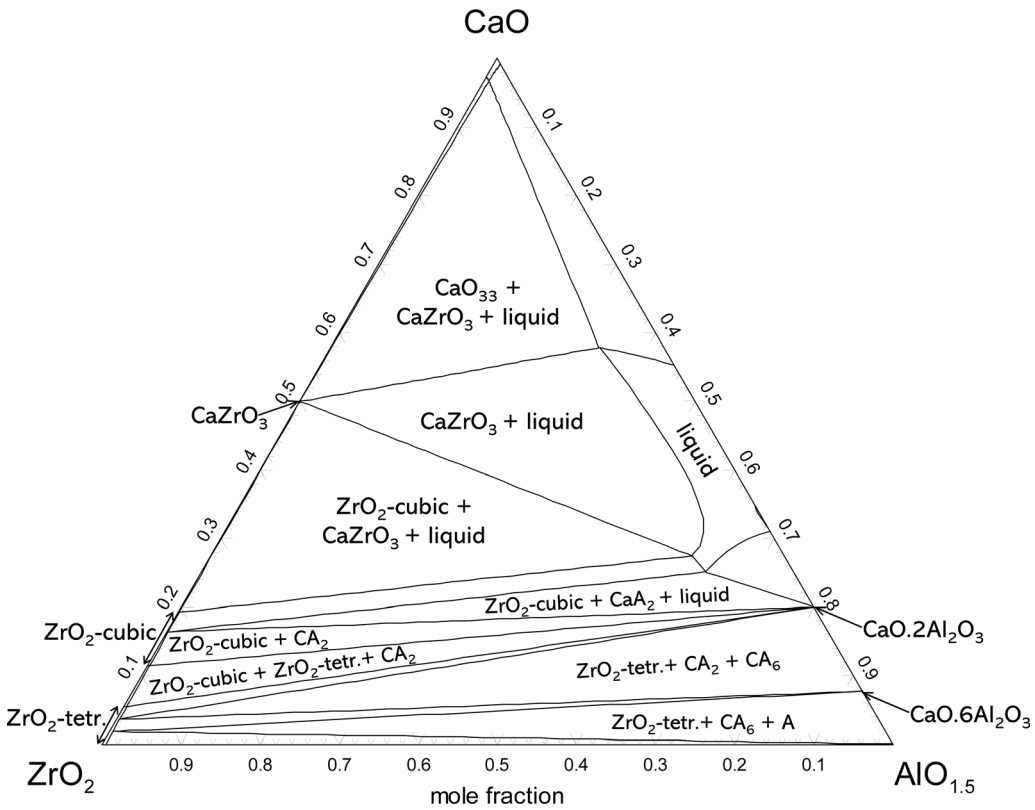

Fig. 8—CaO-ZrO_2-$AlO_{1.5}$ phase diagram at 1873 K (1600 °C) drawn using FactSage[12]

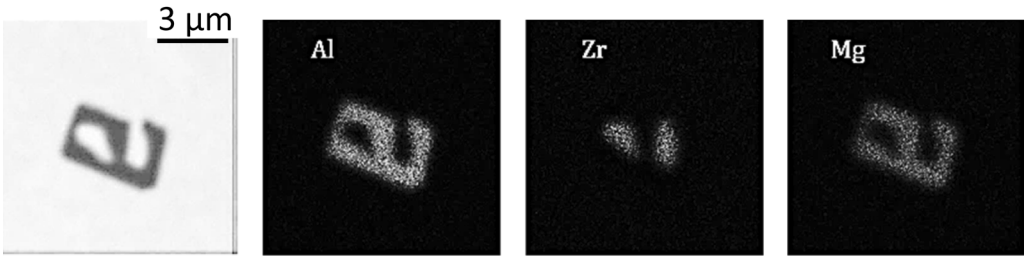

Fig. 9—Inclusion with ZrO_2 in core, observed from the steel sample taken 90 min after Al addition, for reaction of Al-killed steel with $CaO-Al_2O_3$ slag in a ZrO_2 crucible. Backscattered electron image, with EDS elemental maps.

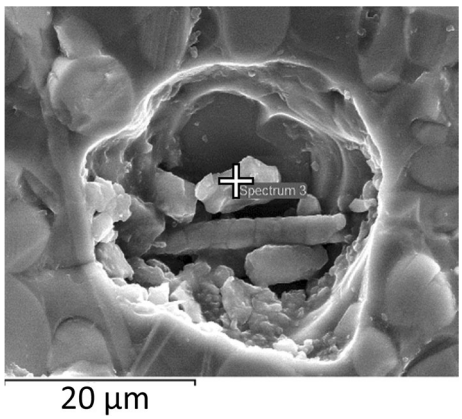

Fig. 10—Slag attack on wall of ZrO_2 crucible that contained Al-killed steel and $CaO-Al_2O_3$ slag (secondary electron micrograph). Micro-analysis showed the particle marked with a cross to have the $CaO-Al_2O_3$ slag composition.

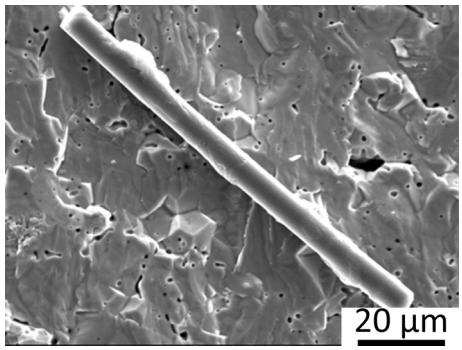

Fig. 11—Si-Ca-Mg-Al-O fiber found on ZrO_2 crucible after reaction with Al-killed steel.

IV. CONCLUSIONS

1. Induction-furnace experiments were designed to clarify the effect of silicon addition on the calcium modification of spinel inclusions by steel–slag reaction. The use of high-purity (electronic grade) silicon clarified that the source of calcium can be steel–slag reactions in addition to calcium impurities in ferrosilicon, for Al-killed steel in contact with $CaO-Al_2O_3-MgO$ slag.
2. There was no significant calcium transfer from $CaO-Al_2O_3-MgO$ slag to alumina inclusions in Al-killed steel not containing added Si, contained in an MgO crucible. Limited calcium transfer to alumina inclusions was observed when the steel was contained in a ZrO_2 crucible instead of MgO crucible. Crucible fines were observed to contribute to $ZrO_2-Al_2O_3$ inclusion formation for steel contained in a ZrO_2 crucible.
3. For reaction of Al-killed steel not alloyed with Si, the largest extent of Ca pick-up was observed when using CaO-3 pct ZrO_2 crucibles. The calcium transfer occurred due to both steel–slag and steel–crucible reactions.

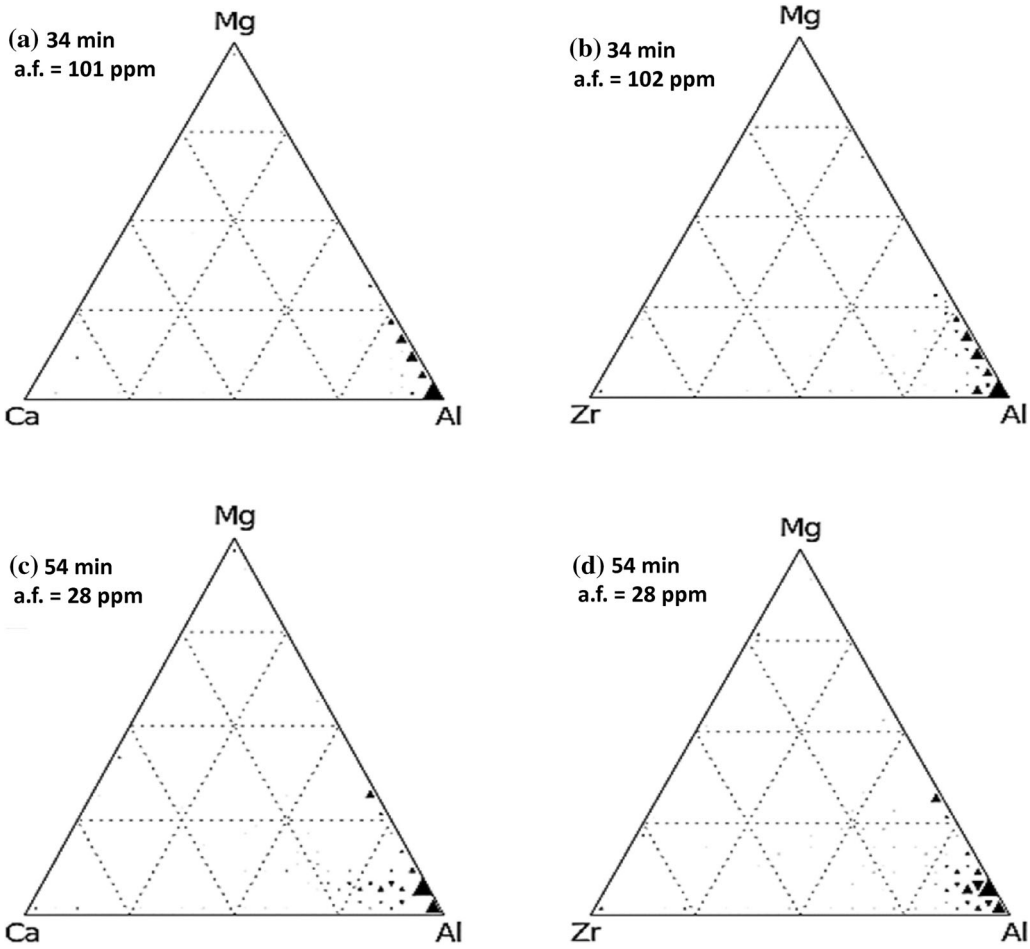

Fig. 12—Change in inclusion content and composition observed during reaction of Al-killed steel with $CaO-Al_2O_3$ slag in a CaO-3 pct ZrO_2 crucible, for samples taken at two different times and showing two different inclusion cation distributions for each: (*a*) Ca-Al-Mg diagram at 34 min; (*b*) Zr-Al-Mg diagram at 34 min; (*c*) Ca-Al Mg diagram at 54 min; (*d*) Zr-Al-Mg diagram at 54 min.

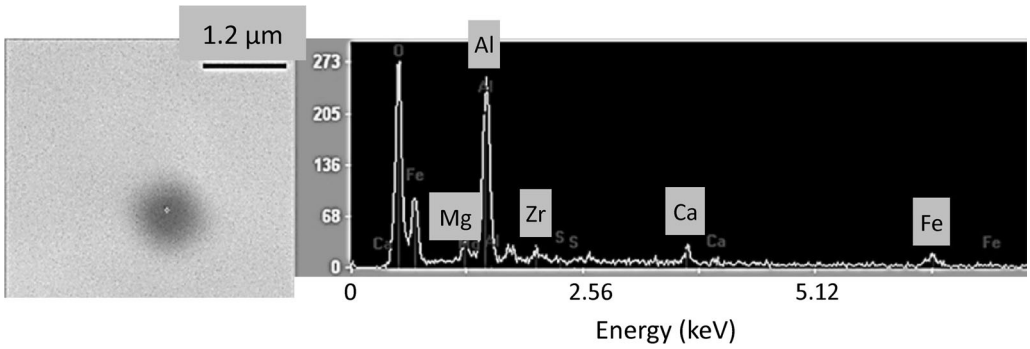

Fig. 13—Calcium-containing inclusion, observed in sample taken at 34th minute during experiment-4.

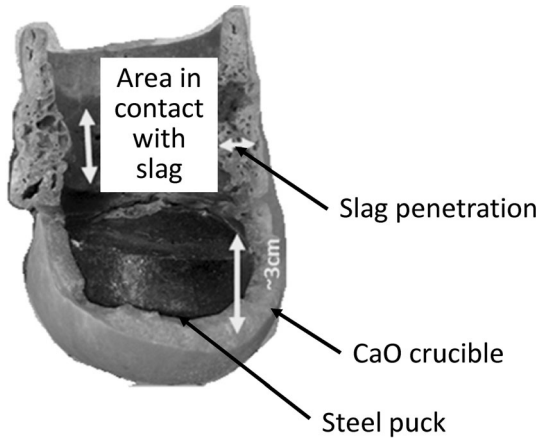

Fig. 14—CaO-3 pct ZrO_2 crucible after the experiment with Al-killed steel and CaO-Al_2O_3, fractured open to show slag penetration into the crucible wall.

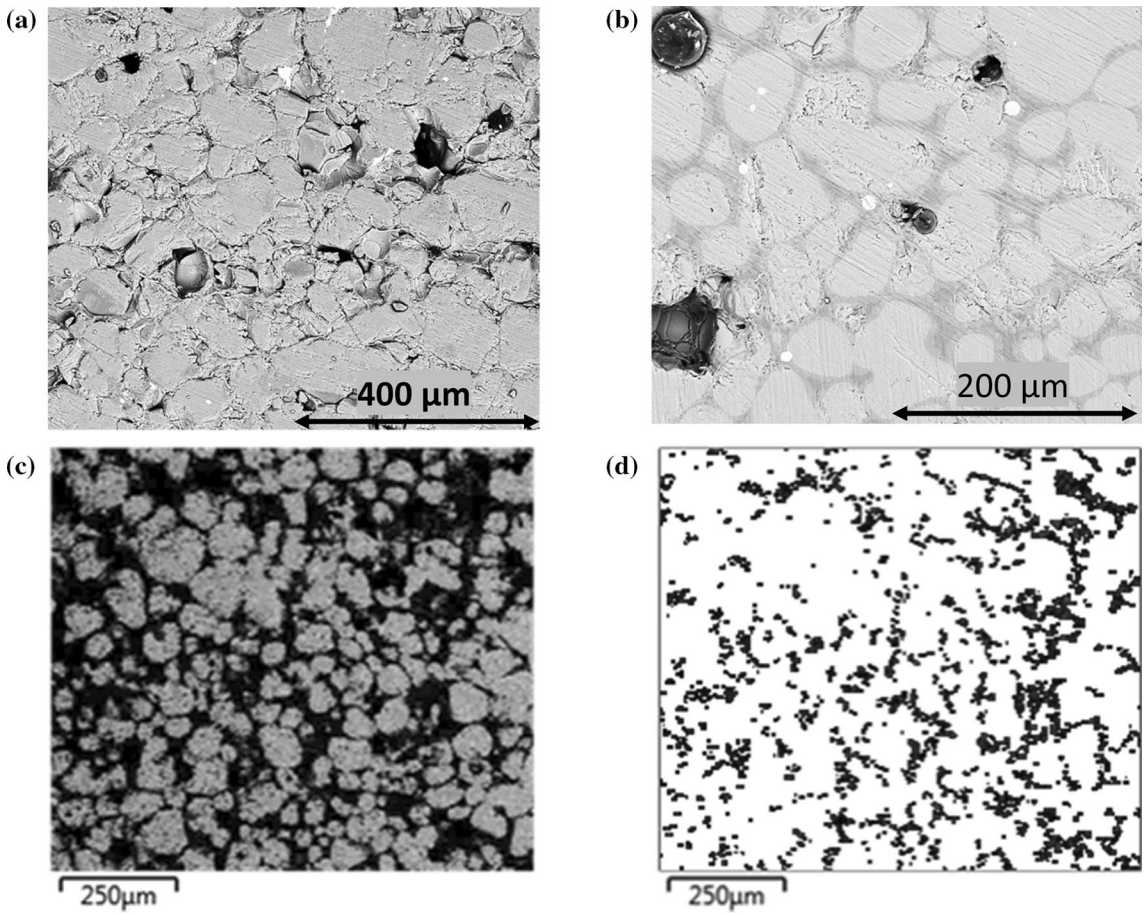

Fig. 15—Images of polished cross-section through a CaO-ZrO_2 crucible in the region penetrated by CaO-Al_2O_3 slag. (*a*) Region near the outside diameter, showing pores and other phases along the grain boundaries (backscattered electron image). (*b*) Slag penetration between grains near the inside diameter (backscattered electron image). EDS map near the inside diameter show (*c*) calcium (brighter areas) and (*d*) aluminum (darker areas).

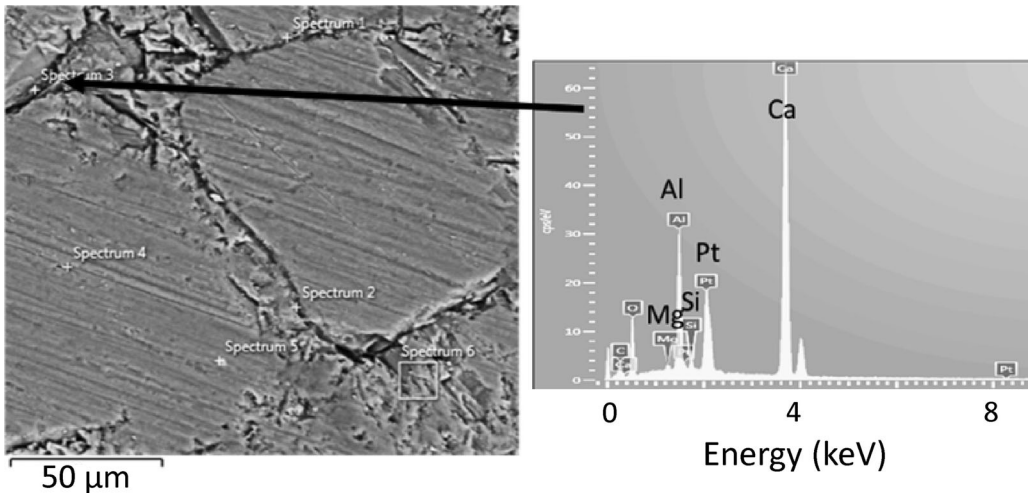

Fig. 16—Presence of Si and Mg in the grain boundary region near the outside diameter of a CaO-3 pct ZrO_2 crucible, shown by EDS analysis.

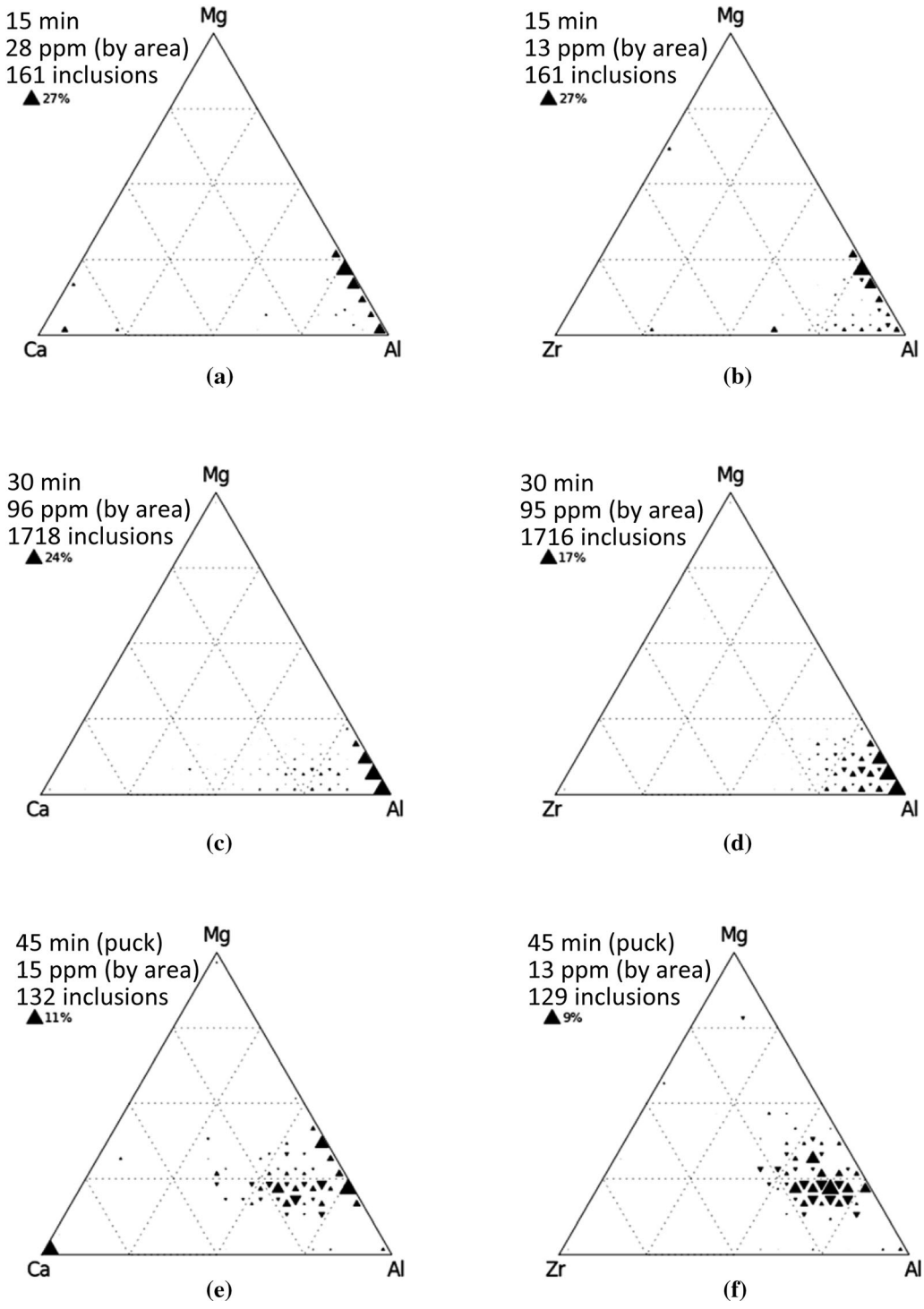

Fig. 17—Inclusion composition change during reaction of Al-killed steel with a CaO-3 pct ZrO_2 crucible, with no added slag. Two inclusion cationic composition distributions are shown for three different times: (*a*) 15 min—Ca-Al-Mg diagram; (*b*) 15 min—Zr-Al-Mg diagram; (*c*) 30 min—Ca-Al-Mg diagram; (*d*) 30 min—Zr-Al-Mg diagram; (*e*) 45 min (bulk metal in crucible)—Ca-Al-Mg diagram; (*f*) 45 min (bulk metal in crucible)—Zr-Al-Mg diagram.

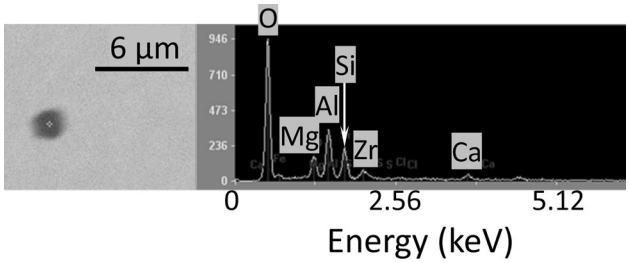

Fig. 18—Calcium-containing inclusion observed in sample taken at the 45th minute from exp-7.7 (CaO crucible, no slag).

ACKNOWLEDGMENTS

The authors acknowledge support from the member companies of the Center for Iron and Steelmaking Research and use of the Materials Characterization Facility at Carnegie Mellon, supported by Grant MCF-677785.

REFERENCES

1. D. Kumar and P. C. Pistorius: Advances in Molten Slags, Fluzes, and Salts: Proceedings of The 10th International Conference on Molten Slags, Fluxes and Salts (MOLTEN16), 2016, pp. 145–54.
2. D. Kumar and P. C. Pistorius: AISTech 2016 – Proceedings of the Iron & Steel Technology Conference, Association for Iron & Steel Technology, Warrandale, PA, 2016, pp. 1151–59.
3. D. Kumar, K.C. Ahlborg, and P.C. Pistorius: *Metall. Mater. Trans. B*, 2019, vol. 50B, pp. 2163–74.
4. C. Liu, D. Kumar, B.A. Webler, and P.C. Pistorius: *Metall. Mater. Trans. B*, 2020, vol. 51B, pp. 529–42.
5. Eugene Pretorius, Nucor Steel, private communications.
6. S.P.T. Piva, D. Kumar, and P.C. Pistorius: *Metall. Mater. Trans. B*, 2017, vol. 48B, pp. 37–45.
7. D. Roy, P.C. Pistorius, and R.J. Fruehan: *Metall. Mater. Trans. B*, 2013, vol. 44B, pp. 1095–1104.
8. D. Tang, M.E. Ferreira, and P.C. Pistorius: *Microsc. Microanal.*, 2017, vol. 23 (6), pp. 1082–90.
9. D. Kumar and P.C. Pistorius: *Metall. Mater. Trans. B*, 2019, vol. 50B (1), pp. 181–91.
10. H. Mu, T. Zhang, R.J. Fruehan, and B.A. Webler: *Metall. Mater. Trans. B*, 2018, vol. 49B (4), pp. 1665–74.
11. S. Yang, Q. Wang, L. Zhang, J. Li, and K. Peaslee: *Metall. Mater. Trans. B*, 2012, vol. 43B (4), pp. 731–50.
12. C.W. Bale, E. Bélisle, P. Chartrand, S.A. Decterov, G. Eriksson, A.E. Gheribi, K. Hack, I.-H. Jung, Y.-B. Kang, J. Melançon, A.D. Pelton, S. Petersen, C. Robelin, J. Sangster, P. Spencer, and M.-A. Van Ende: *CALPHAD*, 2016, vol. 54, pp. 35–53.
13. S. Spooner, Z. Li and S. Sridhar: Scientific Reports, 2017, vol. 7, Article Number 5450.